THE ASTROPHYSICAL JOURNAL, 430:L125–L128, 1994 August 1

THE MOLECULAR CONTENT OF THE ROSETTE'S TEARDROPS

E. GONZÁLEZ-ALFONSO[1,2] AND J. CERNICHARO[2]
Received 1993 March 23; accepted 1994 March 9

ABSTRACT

We report the detection of the $J = 1 \rightarrow 0$ and $J = 2 \rightarrow 1$ lines of ^{12}CO and ^{13}CO, and of the $J = 2 \rightarrow 1$ and $J = 3 \rightarrow 2$ lines of CS, in the direction of the small teardrops of the Rosette nebula. These objects appear in the optical as dark patches of 3″–30″ diameter against the bright H II region of the Rosette nebula. The CO lines were detected in all the observed globules. One of the observed teardrops is still connected to a large elephant trunk by a tenuous filament, which has also been detected in ^{12}CO. The sizes of the ^{12}CO $J = 2 \rightarrow 1$ emitting regions are found to be similar to the optical sizes. The kinetic temperature of the globules is 15–20 K, and the beam-averaged molecular hydrogen densities inferred from the ^{13}CO lines range from 2×10^3 to 7×10^3 cm^{-3}. CS $J = 2 \rightarrow 1$ emission was detected toward two small teardrops and marginally toward another one. The CS $J = 3 \rightarrow 2$ line was detected in one of the above globules. Analysis of these lines yields to an upper limit of the density of $(1–3) \times 10^4$ cm^{-3} for this teardrop. The masses range from $\sim 0.02\ M_\odot$ for a well-isolated and defined teardrop to $\sim 0.5\ M_\odot$ for one which is still connected to a larger globule. Visual extinctions are also very low with typical values of $\sim$1–3 mag.

Subject headings: H II regions — ISM: general — ISM globules — ISM: individual (Rosette nebula) — ISM: molecules

1. INTRODUCTION

Speck globules, also known as "teardrops" (Herbig 1974), are among the smallest and best defined objects found in the interstellar medium. Their sizes range from 3″ to 30″. They are seen against the bright background of some H II regions, normally surrounding larger gas and dust condensations. In particular, these globules are found to be numerous around the elephant trunks (ETs) in the northwest quadrant of the Rosette nebula (RN), suggesting a close association to them. The ETs are blueshifted in velocity relative to the central cluster of ionizing stars in the nebula and seem to be the residual of an expanding shell driven by the stellar winds (Schneps, Ho, & Barret 1980). The expanding velocity of the globules is ~ 20 km s^{-1}.

The only preliminary study of the teardrops (TDRs) is that of Herbig (1974) (see his Plate II) who determined their sizes from an optical plate and discussed their possible origin and age. They have an elongated shape pointing toward the ionizing stars of the RN, which suggests that the evolution of the TDRs is strongly affected by the UV and/or winds from these stars. The lack of radio observations is undoubtedly due to the small size of the TDRs, significantly smaller than most of the single radio telescope beams. In addition to that, since the TDRs are directly exposed to the stellar winds and to strong UV radiation from the center of the RN, the presence of molecules in these objects could seem to be, in principle, rather unlikely.

We present the first radio observations of four of the smallest TDRs of the RN in the two lowest rotational transitions of ^{12}CO and ^{13}CO. The ^{12}CO and ^{13}CO lines were detected in all the observed globules. We also report the detection of the CS $J = 2 \rightarrow 1$ line toward two of the above TDRs and marginally toward another one, and of the CS $J = 3 \rightarrow 2$ line toward one of them. Our main goal has been to derive the physical conditions characterizing these small objects, and their dynamical status.

2. OBSERVATIONS AND RESULTS

All the observations were carried out with the IRAM 30 m telescope on Pico Veleta (Spain) in three different periods: 1990 June, 1992 September, and 1993 June. The ^{12}CO $J = 1 \rightarrow 0$ and $J = 2 \rightarrow 1$ lines were observed simultaneously by using two SIS receivers at wavelengths of 3 and 1 mm. The beamwidth of the telescope is 12″ at 230 GHz and 22″ at 115 GHz. Typical SSB system temperatures were of 700 K for the 3 mm receiver and 1000 K for the 1.3 mm receiver. The spectrometer consisted of two filterbanks of 256×1 MHz channels and 256×100 kHz. The velocity resolution provided by the 100 kHz filters was 0.26 km s^{-1} for the $J = 1 \rightarrow 0$ line and 0.13 km s^{-1} for the $J = 2 \rightarrow 1$ line.

A raster procedure, with three ONs per OFF spaced by 6″, was used to map the globules in the ^{12}CO lines. The reference position was taken at the center of the RN, which has no noticeable CO emission (even in the $J = 1 \rightarrow 0$ line of ^{12}CO which could be contaminated by H38α emission). Pointing was checked every hour, and pointing errors never exceeded 3″ during our observations. Several rasters were done in each globule. The final noise in individual CO spectra was 0.1–0.3 K ($1\ \sigma$) giving typical signal-to-noise ratios of 5 in positions near the globule edges and of 40 in the central regions. Antenna temperature corrected for atmospheric absorption was obtained from two absorbers at ambient and liquid nitrogen temperatures. In order to get homogeneous calibrations for each globule, their center positions were observed every hour. The results were consistent within 15%. The ^{13}CO lines were observed toward only one to two positions on each globule, and the CS lines were observed toward the CO peak emission position of three of the TDRs. As the observed objects are smaller than the telescope beam, the relevant temperature scale is main beam temperature, which was obtained by dividing the antenna temperature corrected for atmospheric absorption,

[1] Postal address: Universidad de Alcalá de Henares, Departamento de Física, Campus Universitario, 28871 Alcalá de Henares, Spain.
[2] Centro Astronómico de Yebes (IGN), Apartado 148, 19080 Guadalajara, Spain.

T_A^*, by the main beam efficiency of the telescope, which is 0.65, 0.5, and 0.45 at 3, 2, and 1.3 mm wavelengths, respectively. Table 1 gives the approximate optical sizes derived from Herbig's plate. From these sizes, and assuming uniform brightness sources, we have calculated the dilution factor for each globule. Some preliminary results for the TDRs were already presented by Cernicharo (1991).

Typical observed ^{12}CO, ^{13}CO $J = 2 \rightarrow 1$, and CS $J = 2 \rightarrow 1$ spectra are shown in Figure 1. Figure 2 shows the integrated ^{12}CO $J = 2 \rightarrow 1$ line intensity contour maps of the observed TDRs. Some spectra show an asymmetric profile, with the blue half of the line more intense than the red one. In the case of TDR 4 two velocity components, at -3.4 and -3.9 km s^{-1}, are observed. The spectra shown in Figure 1 for TDR 10 correspond to the head of the globule. The similar ^{12}CO and ^{13}CO ($2 \rightarrow 1$) profiles in TDR 10 marginally exhibit an asymmetric shape. Although this is not obvious in the profiles of Figure 1, the same tendency (blue emission enhanced over red) is found across most of the head of TDR 10 and the main body of TDR 13. The CS ($2 \rightarrow 1$) line profile in TDR 10 peaks at about the center of the CO lines. In addition to the asymmetric profiles, some CO spectra show the presence of blue wings. Where red wings are detected, they are less intense than the blue wings. No bipolar structure of the wings is apparent in TDR 10, which is resolved at 1.3 mm wavelength, but more sensitive observations are necessary to confirm this fact. The wings cover a velocity range of ~ 1 km s^{-1} and do not have any preferential spatial location in the globules. The wings are observed mainly in the $J = 2 \rightarrow 1$ line of ^{12}CO. The $J = 1 \rightarrow 0$

TABLE 1

OPTICAL SIZES, LINE PARAMETERS, AND PHYSICAL PARAMETERS OF THE TEARDROPS

Globule	TDR 4	TDR 10	TDR 13	TDR 20
Size axis 1[a]	13″	25″	14″	11″
Size axis 2[a]	11″	15″	14″	8″
V_{LSR} (km s^{-1})	−3.8	0.5	−1.4	−1.2
$T_{MB}^{12}(1-0)$[b] (K)	2.6	6.7	5.1	1.8
$T_{MB}^{12}(2-1)$[b] (K)	6.9	13.6	8.5	4.4
$T_{MB}^{13}(1-0)$[b] (K)	0.15	1.5	0.6	0.3
$T_{MB}^{13}(2-1)$[b] (K)	...	4.0	2.3	0.9
$\Delta V(^{13}\text{CO } 2-1)$ (km s^{-1})	0.54	0.94	0.71	0.79
T_{MB} (CS 2–1) (K)	...	0.54	0.36	0.40
T_{MB} (CS 3–2) (K)	...	0.38	<0.26	<0.54
ΔV (CS 2–1) (km s^{-1})	...	0.50	0.46	0.29
$T_k^{(10)}$ (K)[c]	14.8	17.5	20.5	15.6
$T_k^{(21)}$ (K)[c]	16.7	21.1	17.7	15.7
$N(^{13}\text{CO})$ (10^{15} cm^{-2})	0.44	3.4	1.6	1.5
$n(\text{H}_2)$[d] (10^3 cm^{-3})	...	3.3	6.7	2.3
M ($M_\odot$)	0.02	0.48	0.11	0.05
t_{ph}[e] (10^4 yr)	0.7	4.4	5.0	1.3
$N(\text{H}_2)$ (10^{21} cm^{-2})	0.3	2.4	1.1	1.1
A_V[f] (mag)	1.3	3.4	2.1	2.1

[a] Approximate optical sizes are given for the two main axis of the globules.

[b] $T_{MB}^{12}(1-0)$, $T_{MB}^{12}(2-1)$, $T_{MB}^{13}(1-0)$, and $T_{MB}^{13}(2-1)$ are the main beam temperatures of the ^{12}CO and ^{13}CO $J = 1-0$ and $J = 2-1$ lines.

[c] Derived kinetic temperatures from the CO(1–0) (10) and CO(2–1) (21) spectra assuming thermalization.

[d] Densities are inferred from the ^{13}CO data.

[e] t_{ph} is the photo-evaporation time of the TDR.

[f] Visual extinctions are derived using the $^{13}\text{CO}/A_V$ relations from Cernicharo & Guélin 1987 and Bachiller & Cernicharo 1986. A cutoff of 1 mag for $^{13}\text{CO}/A_V$ has been adopted.

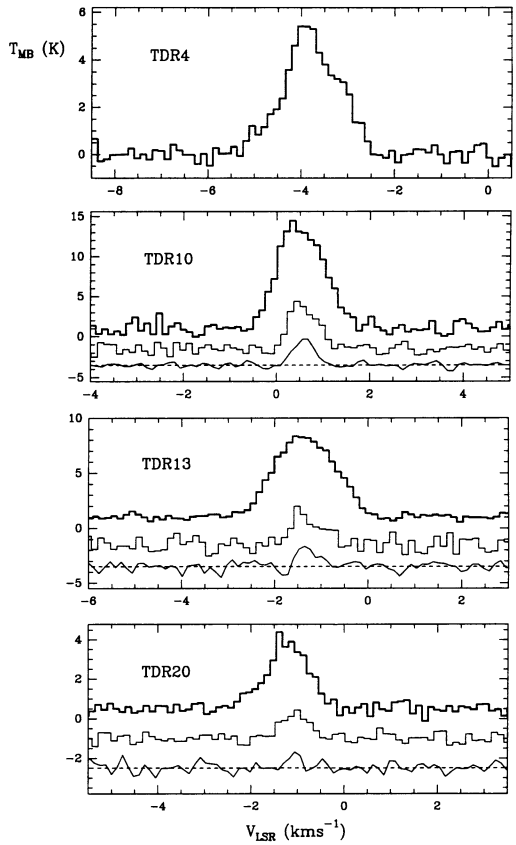

FIG. 1.—Observed ^{12}CO $J = 2 \rightarrow 1$ (*thick histogram*), ^{13}CO $J = 2 \rightarrow 1$ (*thin histogram*), and CS $J = 2 \rightarrow 1$ (*thin line*) spectra toward the teardrops. The ^{13}CO line intensities have been multiplied by 2 and the CS ones by 6, 8, and 2 in the three lower panels, respectively.

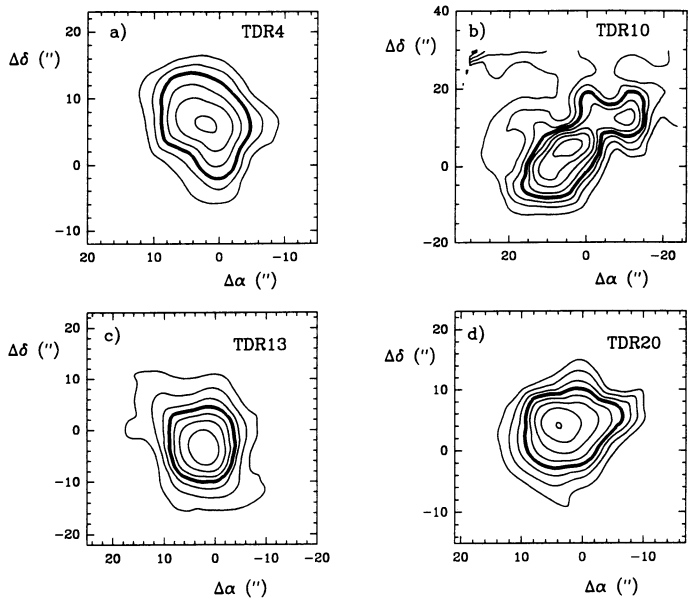

FIG. 2.—Integrated intensity contour maps in the ^{12}CO $J = 2 \rightarrow 1$ line of the teardrops. Thick contours correspond to half-power intensity. In TDR 10 the emission toward the north comes from the filament which connects the globule to an elephant trunk. Reference positions, first contours and steps are (*a*) $\alpha_{1950} = 6^h28^m45^s.50$, $\delta_{1950} = 5°28'45''.5$, 3 and 2 K km s^{-1} (*b*) $\alpha_{1950} = 6^h28^m30^s.56$, $\delta_{1950} = 5°08'24''.5$, 2 and 1.5 K km s^{-1}; (*c*) $\alpha_{1950} = 6^h28^m16^s.71$, $\delta_{1950} = 5°07'59''.5$, 1.5 and 2 K km s^{-1}; (*d*) $\alpha_{1950} = 6^h28^m03^s.99$, $\delta_{1950} = 5°10'49''.2$, 0.5 and 0.5 K km s^{-1}.

lines also show similar wings, but dilution effects decrease their intensity and the signal to noise ratio is poorer. The possible contamination of the ^{12}CO $J = 1 \rightarrow 0$ line by H38α emission is below our sensitivity limit.

Table 1 gives the line parameters of the spectra observed toward the central position of the TDRs together with the physical parameters deduced from them. The two values of the kinetic temperature given in this table are obtained from the peak temperatures of the ^{12}CO $J = 1 \rightarrow 0$ and $J = 2 \rightarrow 1$ lines, corrected for beam dilution and by assuming thermalization of the lines. In view of the uncertainties in the dilution factors, the agreement between both values is reasonably good, and both transitions can be considered thermalized at $\sim$15–20 K. The values of the column density $N(^{13}CO)$ and the density $n(H_2)$ have been derived from the ^{13}CO $J = 1 \rightarrow 0$ and $J = 2 \rightarrow 1$ data using a large velocity gradient code (LVG) for the calculations with the collisional rates of Schinke et al. (1985). We have assumed the same dilution factors for ^{13}CO and ^{12}CO emission. Toward TDR 4 the ^{13}CO $J = 1 \rightarrow 0$ line was marginally detected at a 3 σ level and the $J = 2 \rightarrow 1$ line was not observed. Assuming a size for TDR 4 of 8.5×10^{-2} pc (11″ at 1600 pc, which is the distance to the RN we have adopted: Turner 1976; Pérez, The, & Westerlund 1987), the resulting $n(H_2)$ is $\sim 0.8 \times 10^3$ cm^{-3}. At these densities, the assumption of equal excitation temperatures for both isotopes is not valid, and the ^{13}CO $J = 1 \rightarrow 0$ opacity is certainly underestimated. The masses are obtained from the $N(H_2)$ data and sizes in Table 1, assuming an ellipsoidal geometry for the globules. Our results indicate molecular hydrogen densities for the observed globules in the range $n(H_2) \sim 1$–7×10^3 cm^{-3} and ^{13}CO column densities in the range N (^{13}CO) = 0.4–3.4×10^{15} cm^{-2}. From the ^{13}CO abundance determinations of Cernicharo & Guélin (1987) and Bachiller & Cernicharo (1986), the corresponding visual extinctions are $\sim$1–3 mag (see Table 1).

In TDR 10 both CS $J = 2 \rightarrow 1$ and $J = 3 \rightarrow 2$ were detected, so an estimate for N(CS) and $n(H_2)$ can be obtained. After correcting for beam dilution we get $n(H_2) = 1$–3×10^4 cm^{-3} and n(CS) $\sim 10^{13}$ cm^{-2}. For the other two TDRs where only CS $J = 2 \rightarrow 1$ is detected (detection in TDR 20 is at a 3 σ level), we can only obtain upper limits for $n(H_2)$. However, due to relatively high noise level in the CS $J = 3 \rightarrow 2$ line spectra toward the later TDRs, we get upper limits of $\sim 10^{5-6}$ cm^{-3}, which do not give further significant information. In these calculations we have also assumed that the CS-emitting regions are equal to the optical sizes. For TDR 10, the inferred $n(H_2)$ is almost one order of magnitude greater than that derived from the ^{13}CO data. The main source of uncertainty in our calculations is the size of the CS and ^{13}CO-emitting regions. If the CS sizes were smaller than those assumed, the ratio T_B(CS $2 \rightarrow 1$)/T_B(CS $3 \rightarrow 2$) would be higher than our derived values, further decreasing the estimates or upper limits for $n(H_2)$. The same applies to the ^{13}CO lines, but a ^{13}CO size is expected to be larger than the CS one, due to more efficient ^{13}CO self-shielding against the UV radiation field from the center of the nebula. Nevertheless, the ratio $N(^{13}CO)/N(CS)$ is in rough agreement with the standard values found in the interstellar medium.

The close agreement between the projected velocities of the ETs (Schneps et al. 1980) and of the TDRs (Fig. 1; Table 1) indicates a true association, so that their common location is definitely more than a chance projection. However, not all of these globules have the same level of association with the ETs. While some TDRs appear to be relatively isolated from these larger condensations, others appear to be closely related to them. TDR 10 is still connected to one of the ETs by tenuous filaments (see Herbig 1974, Plates 1 and 2). This ET was observed by Schneps et al. (1980) and labeled in their paper as globule "D." The velocity they derived for it was in the range 0.2–0.8 km s^{-1}. Figure 2*b* shows that the emission peak of TDR 10 in the ^{12}CO $J = 2 \rightarrow 1$ line is at the head of the TDR ($\Delta\alpha = 6''$, $\Delta\delta = 6''$). Nevertheless, the emission extends beyond the north of the head, corresponding to the joining filament visible at optical wavelengths. In this region the emission intensity is weaker and extended. Figure 3 shows the ^{12}CO $J = 2 \rightarrow 1$ line intensity contour maps integrated over different velocity intervals. A velocity gradient between the gas in the filament and in the head of TDR 10 is clearly present. No velocity gradient is found at the head. Thus, the gas in the filament is blueshifted relative to both the gas in TDR 10 and in globule D. The spectra along this filament become broad and non-Gaussian and present two well-defined velocity components in some directions. The relative intensity of the red and blue halves of the line changes with position: the blue emission is stronger at the north of the filament for the range of declination we mapped.

TDR 4, TDR 13, and TDR 20 are relatively isolated and elongated TDRs, which in the optical appear to point to the center of the RN (see Herbig 1974, Plates 1 and 2). This orientation is apparent in ^{12}CO ($2 \rightarrow 1$) intensity contour maps of TDR 4 and TDR 20 (Figs. 2*a* and 2*d*) and only marginal in that of TDR 13 (Fig. 2*c*).

3. DISCUSSION

As pointed out above, Herbig (1974) found some TDRs in the RN still connected to the ETs by tentacles of dust and gas

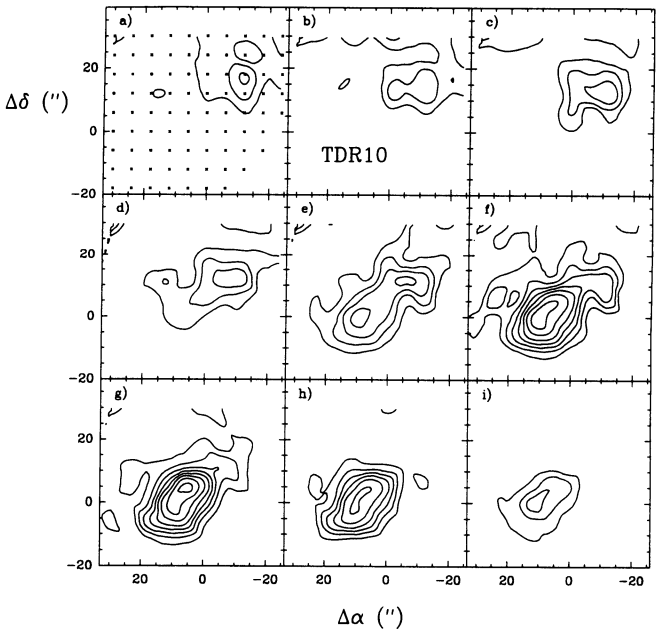

FIG. 3.—^{12}CO $J = 2 \rightarrow 1$ emission in TDR 10 integrated over different velocity intervals. First contours are 0.6 K km s^{-1} and steps are 0.5 K km s^{-1}. The observed positions are marked in the first panel. Velocity intervals are (*a*) -1.4 to -1.1 km s^{-1} (*b*) -1.1 to -0.8 km s^{-1}, (*c*) -0.8 to -0.5 km s^{-1}, (*d*) -0.5 to -0.2 km s^{-1}, (*e*) -0.2 to 0.1 km s^{-1} (*f*) 0.1 to 0.4 km s^{-1}, (*g*) 0.4 to 0.7 km s^{-1}, (*h*) 0.7 to 1.0 km s^{-1}, and (*i*) 1.0 to 1.3 km s^{-1}.

and suggested that the TDRs are fragments of the large ETs in the nebula. We have observed one of these small globules in the CO lines (TDR 10), and we have also detected the filament. No velocity gradient has been found across the head of the globule, but the gas in the filament is blueshifted relative to the gas in the head and in the ET. This may be associated with the curvature which this filament exhibits in the optical images and suggests its disruption is surely caused by the action of stellar winds and/or UV radiation. The CO spectra are broad, and emission is found in a range of ~ 3 km s^{-1}. This fits a picture in which stellar winds and/or UV radiation accelerate and disperse the gas of the tentacle in the outward direction. The final stage of this process should be the total dispersion and photoionization of the arm, and the appearance of TDR 10 as a small and isolated teardrop. The small and diffuse tails of some TDRs should be considered as the shadowed part of the tentacle(s) linking the TDR to the parent globule.

The TDRs of the RN are not gravitationally bound. The gravitational virial mass derived for a globule which subtends 13″ at 1600 pc (~ 0.05 pc) with a ^{13}CO line FWHM of 0.7 km s^{-1} is somewhat greater than 5 $M_\odot$ and is even larger if the linewidth of ^{12}CO is used for this equilibrium calculation. This value is one to two orders of magnitude greater than the masses of the TDRs derived in the previous section, so they cannot be confined by their own gravity. Average molecular hydrogen densities higher than 10^5 cm^{-3} would be necessary to bind such small structures. CS observations toward TDR 10 give also significantly lower densities, also when compared with those found in other small cometary globules like ORI-I-2 (Cernicharo et al. 1992) or IC 1396 (Duvert et al. 1990). If the CS emission comes from a smaller region than CO, as is suspected from the relative CS–CO linewidth (which cannot be explained by opacity effects), the derived densities could be considered as upper limits because the $J = 3$–2 to $J = 2$–1 line intensity ratio will decrease due to the different beam dilution. Hence, the gravitational energy should be even lower in this case. However, the globules are directly exposed to UV radiation from the central star cluster, which can provide the external pressure necessary to confine them.

The line wings in the ^{12}CO profiles could be also explained in terms of the ionized gas pressure exerted on the neutral gas. Blue wings are more intense and extended than red wings, and no bipolar structure is apparent from our data (however, our angular resolution is poor and no definitive conclusion about the structure can be attained). Since no energetic source is expected to be in the inner regions of the TDRs, we associate this blue and red emission to the dynamics of the gas on their surface. The enhanced blue wings could represent molecular material which expands in the direction of the tail, leading to the observed teardrop shape of the globules. As pointed out above, another possibility is that the wings are associated with the pressure that the ionized gas exerts on the neutral gas, which is accelerated toward the observer in a thin shocked layer. If this layer is not resolved by our beam and/or is optically thin, it should give rise to ^{12}CO emission with a line wing semblance. In fact, the physical conditions we get for the TDRs are compatible with the presence of a shock front advancing into the globules, because the conditions of the ionization front at the TDRs location are expected to be M-type (e.g., Bertoldi 1989). On the other hand, the central part of the CO profiles does not show, except in the case of TDR 4, any clear separation of the molecular emission in different velocity components. Although some asymmetry is found in the CO profiles, the CS lines (when detected) peak at about the symmetry center of the CO lines.

An important parameter for the TDRs is their age of survival against evaporation. From the physical parameters in Table 1 we can estimate their lifetime (see, e.g., Reipurth 1983). It is typically a few times 10^4 yr (see Table 1), which is much shorter than the life of the Rosette nebula (4–7×10^5 yr: Schneps et al. 1980; Matthews 1967). The TDRs seem to be at different evolutionary stages as some of them are completely isolated while others are still connected to the ETs through tenuous filaments. It is suggestive to conclude that the TDRs are continuously being created from the large structures of molecular gas present in this complex.

We wish to thank A. Barcia, R. Bachiller, P. Planesas, and D. Downes for critical reading and useful comments of the manuscript. We also thank the IRAM staff on Pico Veleta for kind hospitality and assistance during the observations. This work has been partially supported by DGCICYT under project number PB 90-408.

REFERENCES

Bachiller, R., & Cernicharo, J. 1986, A&A, 166, 283
Bertoldi, F. 1989, ApJ, 346, 735
Cernicharo, J. 1991, in The Physics of Star Formation and Early Stellar Evolution, ed. C. J. Lada & N. D. Kylafis (Dordrecht: Kluwer), 287
Cernicharo, J., Bachiller, R., Duvert, G., González-Alfonso, E., & Gómez-González, J. 1992, A&A, 261, 589
Cernicharo, J., & Guélin, M. 1987, A&A, 176, 299
Duvert, G., Cernicharo, J., Bachiller, R., & Gómez-Gonzalez, J. 1990, A&A, 233, 190
Herbig, G. H. 1974, PASP, 86, 604
Matthews, W. 1967, ApJ, 147, 965
Pérez, M. R., The, P. S., & Westerlund, B. E. 1987, PASP, 99, 1050
Reipurth, B. 1983, A&A, 117, 183
Schinke, R., Engel, V., Buck, U., Meyer, H., & Diercksen, G. H. F. 1985, ApJ, 299, 939
Schneps, M. H., Ho, P. T. P., & Barret, A. H. 1980, ApJ, 240, 84
Turner, D. G. 1976, ApJ, 210, 65